

A novel energy-efficient rotational variable stiffness actuator

Shodhan Rao, Raffaella Carloni and Stefano Stramigioli

Abstract—This paper presents the working principle, the design and realization of a novel rotational variable stiffness actuator, whose stiffness can be varied independently of its output angular position. This actuator is energy-efficient, meaning that the stiffness of the actuator can be varied by keeping constant the internal stored energy of the actuator. The principle of the actuator is an extension of the principle of translational energy-efficient actuator vsaUT. A prototype based on the principle has been designed, in which ball-bearings and linear slide guides have been used in order to reduce losses due to friction.

I. INTRODUCTION

Two of the most important medical applications where there is interaction between robotic devices and humans are prosthesis and rehabilitation. The prosthetic and wearable robots used in these applications are usually devices whose stiffness remains constant during operations. In contrast, a healthy human performs various tasks like grasping, manipulation, walking etc. by skillfully adapting the stiffness of various joints in order to optimize the task. It has been shown in [1] that it is possible to decode intended position and stiffness of the wrist joint using EMG signals from the forearm. If one can design a joint, whose position and stiffness can be automatically varied, then using a neural signal decoding unit, it is possible to design a prosthetic device whose position and stiffness can be varied as desired by its owner. Such a prosthetic device is capable not only of giving a much more natural feel to the user, but also of interacting safely with the environment. The joints for such prosthetic devices can be realized using a class of actuators known as *variable stiffness actuators*, whose stiffness can be controlled independently of their output position.

A detailed review of most of the variable stiffness actuators that have been developed so far, is given in [2]. In a variable stiffness actuator, the stiffness can either be controlled actively by adjusting stiffness during operation using feedback, feedforward and/or adaptive control methods, or it can be a mechanical property of the system, realized passively when the configuration of certain internal springs determines how they are sensed at the output of the actuators. The disadvantages of active stiffness control are that, during impact, the hardware stiffness will be felt and it consumes energy for adjusting stiffness, while if passive elastic elements are present, energy can be stored in them and released again when required.

This work has been partially funded by IMPACT Research Institute of the University of Twente, as part of the project ENERGY EFFICIENT ACTUATIONS, and partially by the European Commission's Seventh Framework Programme as part of the project VIATORS under grant no. 231554.

{s.rao,r.carloni,s.stramigioli}@utwente.nl, Dept. Electrical Engineering, Faculty of Electrical Engineering, Mathematics and Computer Science, University of Twente, 7500 AE Enschede, The Netherlands.

Several variable stiffness actuators rely on pretension of their internal springs to impart output stiffness, and the pretension needs to be changed in order to vary the apparent output stiffness. Thus internal springs of such actuators need to undergo loading/unloading whenever the stiffness of the actuator needs to be changed during operations. As a consequence, the energy stored in the internal springs, which will be henceforth referred to as the internal energy of the actuator, changes whenever its stiffness is varied.

In the context of variable stiffness actuators, an *energy efficient variable stiffness actuator* has been introduced in [3] as one for which the apparent output stiffness can be changed without injecting to or extracting energy from the internal elastic elements. A proof of concept of the same principle including a description of a mechanical design based on the principle and results of experiments carried out on a prototype has been presented in [4]. These results show that the behaviour of the prototype is in accordance with the theoretical results. This further proves that it is possible to realize a variable stiffness actuator, for which the output stiffness can be controlled independently of the output position in such a way that the internal energy does not change.

It can be shown that the actuators presented in [5] and [6] are also energy efficient variable stiffness actuators. The mechanical designs of the actuators presented in [4], [5] and [6] make use of linear springs and the apparent output stiffness of each of these actuators can be varied by varying the length of a lever arm. The main advantage of using an energy efficient variable stiffness actuator over an inefficient one is that there is lesser loading/unloading of internal springs, which implies longer life of springs in the case of the former category of actuators.

This paper presents the design of an *energy efficient rotational variable stiffness actuator*. The apparent output stiffness of the designed actuator can be varied by varying the length of a lever arm, just like in the case of the actuators presented in [4], [5] and [6]. A proof of concept of the actuator is presented in the form of the description of the design of a prototype based on the conceptual design and comparison of the results of experiments on the prototype and theoretical expected results. It is shown that there is good agreement between the two results.

The paper is organized as follows. Section II presents a port-based model of a variable stiffness actuator. Using this model, conditions for energy efficiency of such an actuator is derived as in [4]. Section III presents the working principle of an energy efficient rotational actuator. In Section IV, we discuss the mechanical design and features of a prototype

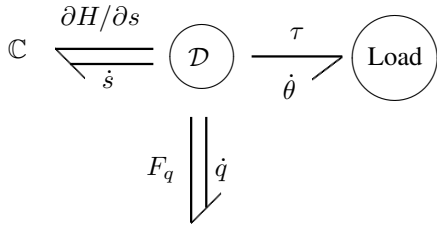


Fig. 1. Generalized model of a variable stiffness actuator - The \mathcal{D} is the Dirac structure, the internal elastic elements are represented by the multidimensional \mathbb{C} -element, described by the energy function H . The internal degrees of freedom are actuated via the control port (\dot{q}, F_q), while the interconnection with the load is via the output port ($\dot{\theta}, \tau$).

of the actuator discussed in Section III. Section V presents experimental results, and the conclusion based on previous sections is presented in Section VI.

II. PORT-BASED MODEL OF A VARIABLE STIFFNESS ACTUATOR

A port-based model of a variable-stiffness actuator has been explained in detail in [3]. Here, we briefly recall the model, in order to understand the condition for energy-efficiency of a variable stiffness actuator.

Port-based modelling is an effective tool in understanding the power flows within a model, and also in deriving conditions for energy-efficiency of a variable stiffness actuator. The following assumptions are made in formulating a port-based model for a variable stiffness actuator:

- the variable stiffness actuator has internal springs,
- there are actuated degrees of freedom, which determine the output stiffness K of the actuator, defined as the partial derivative of the generalized output force τ of the actuator with respect to its generalized output position θ , i.e. $K = \frac{\partial \tau}{\partial \theta}$,
- there is negligible loss of energy due to friction, and inertias of all parts used in the actuator can be neglected,

The port-based model of a variable stiffness actuator is graphically depicted in Fig. 1. This model has three elements, namely the multi-dimensional \mathbb{C} -element, which represents the internal springs, the *load* element and the Dirac-structure \mathcal{D} . The \mathbb{C} -element is characterized by a state vector s , whose elements are the elongations of the internal springs, and by an internal scalar energy function $H(s)$, which denotes the total energy stored in the springs. The Dirac-structure \mathcal{D} has three ports namely the *control port*, the *output port* and the *internal port* and the port variables of each of these ports are described below.

The internal degrees of freedom of the actuator represented by the vector q are actuated via the *control port*. The flow variable of the control port is the rate of change of the configuration variable q , denoted by \dot{q} , and the effort variable of this port is the generalized force that actuates q , denoted by F_q . The effort variable of the output port is the generalized output force τ , and its flow variable is the rate of change of the generalized output position θ , denoted by $\dot{\theta}$. The internal port of the Dirac structure connects it to the multidimensional spring element \mathbb{C} via a power bond. The flow variable of this

port is the rate of change of the state s of the springs, denoted by \dot{s} and its effort variable is the force exerted by the springs, which is equal to the vector $\frac{\partial H}{\partial s}$.

The Dirac-structure \mathcal{D} is power-continuous, and therefore the sum of the powers through all ports of the structure is zero. It can be shown that power continuity of the Dirac structure translates into the following mathematical equation:

$$\begin{bmatrix} \dot{s} \\ F_q \\ \tau \end{bmatrix} = \underbrace{\begin{bmatrix} 0 & A(q, \theta) & B(q, \theta) \\ -A(q, \theta)^T & 0 & 0 \\ -B(q, \theta)^T & 0 & 0 \end{bmatrix}}_{D(q, \theta)} \begin{bmatrix} \frac{\partial H}{\partial s} \\ \dot{q} \\ \dot{\theta} \end{bmatrix}$$

Note that the matrix $D(q, \theta)$ is skew-symmetric and is allowed to depend on both the internal degrees of freedom q and the output position θ . The rate of change of energy stored in the internal springs is

$$\begin{aligned} \frac{dH}{dt} &= \left(\frac{\partial H}{\partial s} \right)^T \frac{ds}{dt} = \left(\frac{\partial H}{\partial s} \right)^T (A(q, \theta)\dot{q} + B(q, \theta)\dot{\theta}) \\ &= -F_q^T \dot{q} - \tau^T \dot{\theta} \end{aligned}$$

which is equal to the sum of the power supplied through the control port and the output port. Observe that

$$\dot{s} = A(q, \theta)\dot{q} + B(q, \theta)\dot{\theta} \quad (1)$$

Note that if $A(q, \theta)$ does not have full rank, then there exist nonzero trajectories q such that $\dot{q} \in \ker(A(q, \theta))$. This implies that if the internal degrees of freedom of the actuator are varied along such trajectories keeping the output position θ constant, then the state s and consequently the energy H stored in the springs remain constant. If in addition, such trajectories of q do change the stiffness of the actuator, then by definition the actuator is energy efficient. Consequently if $\text{nullity}(A(q, \theta)) \neq 0$, and q is such that $\dot{q} \in \ker(A(q, \theta))$, and it leads to change in the stiffness of the actuator when θ is kept constant, then the actuator is energy efficient.

III. CONCEPTUAL DESIGN

We now present the conceptual design of an energy efficient rotational variable stiffness actuator. A schematic of the actuator is given in Fig. 2.

With reference to Fig. 2, S_1 and S_2 are the internal springs of the actuator that are placed in the moving frame $EFGH$; q_1 and q_2 are the actuated internal degrees of freedom of the actuator, whose lengths can be varied using motors M_1 and M_2 , respectively. Point A is a revolute joint whose rotation θ represents the actuator output; BL and CD are linear actuators or slide screws. At points C and D , there are sliders so that the frame $EFGH$ is free to move horizontally with respect to the link CD . B is a revolute joint that is placed on a slider between the two internal springs S_1 and S_2 of the actuator.

It is assumed that the springs S_1 and S_2 are linear. Let k denote the elastic constant of each of the two springs. The force due to the elongation/compression of the springs S_1

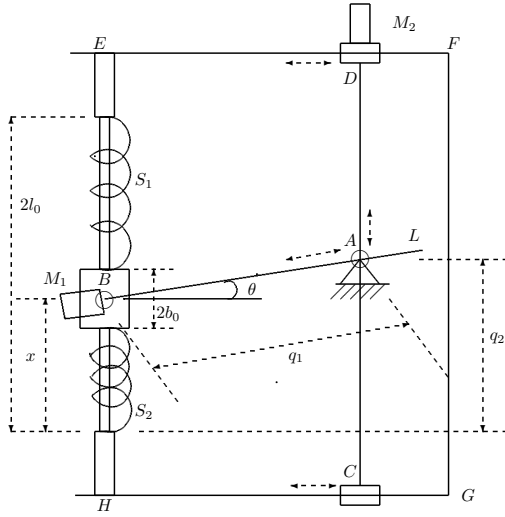


Fig. 2. Schematic of a variable stiffness rotational actuator.

and S_2 acting at point B is given by $F_s = 2k(l_0 - x)$. This implies that the output torque at point A is

$$\tau = F_s q_1 \cos \theta = 2k(l_0 - x) q_1 \cos \theta \quad (2)$$

Observe from Fig. 2 that $x = q_2 - q_1 \sin \theta$. Substituting for x in equation (2), we get

$$\begin{aligned} \tau &= 2kq_1(l_0 - q_2 + q_1 \sin \theta) \cos \theta \\ &= 2kq_1(l_0 - q_2) \cos \theta + kq_1^2 \sin 2\theta \end{aligned}$$

The output stiffness K of the actuator is given by

$$K = \frac{\partial \tau}{\partial \theta} = 2kq_1(q_2 - l_0) \sin \theta + 2kq_1^2 \cos 2\theta \quad (3)$$

Since K depends on the internal degrees of freedom q_1 and q_2 , it follows that the actuator is a variable stiffness actuator. We now prove that it is energy efficient.

The vector q of internal degrees of freedom is given by

$$q = \begin{bmatrix} q_1 \\ q_2 \end{bmatrix}$$

From Fig. 2, it follows that the state s of the springs is given by

$$\begin{aligned} s &= \begin{bmatrix} s_1 \\ s_2 \end{bmatrix} = \begin{bmatrix} 2l_0 - b_0 - x \\ x - b_0 \end{bmatrix} \\ &= \begin{bmatrix} 2l_0 - b_0 - q_2 + q_1 \sin \theta \\ q_2 - q_1 \sin \theta - b_0 \end{bmatrix} \end{aligned}$$

Differentiating the above equation, it follows

$$\dot{s} = \begin{bmatrix} \sin \theta & -1 \\ -\sin \theta & 1 \end{bmatrix} \dot{q} + \begin{bmatrix} q_1 \cos \theta \\ -q_1 \cos \theta \end{bmatrix} \dot{\theta}$$

By comparison with equation (1), it follows that for the actuator,

$$A(q, \theta) = \begin{bmatrix} \sin \theta & -1 \\ -\sin \theta & 1 \end{bmatrix}$$

and $\text{nullity}(A(q, \theta)) = 1$. By varying q such that $\dot{q} \in \ker(A(q, \theta))$, the internal energy of the actuator is not changing while changing the output stiffness, given by (3). It follows that the actuator is energy efficient.

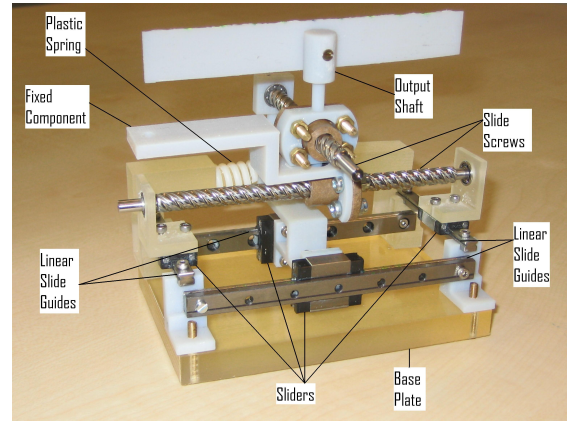


Fig. 3. First view of the prototype.

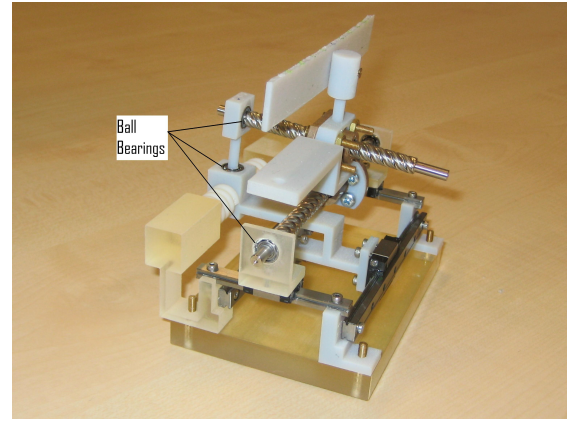


Fig. 4. Second view of the prototype.

IV. PROTOTYPE OF THE ACTUATOR

A mechanical prototype of the rotational variable stiffness actuator has been built based on the principle presented in the previous Section. Two views of the actuator prototype are shown in Fig. 3 and Fig. 4.

Linear slide guides have been used to build the frame $EFGH$ and slide screws have been used to build the linear actuators BL and CD with reference to Fig. 2. Deep-groove ball-bearings have been used to minimize friction between rotating parts and their supports. The remaining materials of the prototype have been built using plastic resins. The prototype has been built without motors, hence it needs to be controlled manually and it serves to illustrate the conceptual design presented in Section III. With reference to Fig. 2, the state $\theta = 0$; $x = l_0$ can be considered as the neutral position of the springs used in the actuator. The linear springs used in the prototype are compression springs made up of plastic resins and these are pre-compressed in their neutral position, so that the effect of both the springs can be felt when the actuator is used.

With reference to Fig. 2, note that the linear actuator BL can be used to vary stiffness by varying q_1 and the linear actuator CD can be used to vary the output angle θ by

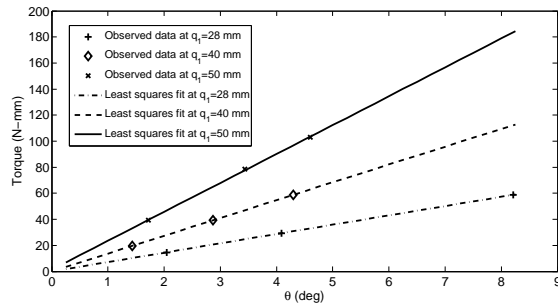


Fig. 5. Graph of output torque τ vs output angular displacements θ at three different values of q_1 .

varying q_2 . In the prototype, the two slide screws can be used to perform these functions. The output angular range of motion that the device can provide is approximately equal to 90° . The length, breadth and height of the prototype are equal to 130 mm, 85 mm and 110 mm, respectively.

V. EXPERIMENTS

Experiments have been performed on the prototype in order to show that its performance is close to the desired performance of the actuator. In Fig. 3, observe that a plastic sheet has been attached to the output shaft. Application of orthogonal forces on this sheet at various distances from the output shaft leads to application of varying torques on the output shaft. In all the experiments that were performed, the internal actuation q_2 with reference to Fig. 2 has been kept constant at l_0 . It should be noted that for the prototype the minimum and maximum values of the actuation q_1 are respectively equal to 28 mm and 50 mm.

The experiments consisted of three phases. In the first phase, with $q_1 = 28$ mm, the output angle θ in response to three different values of torques on the output shaft were measured. In the remaining two phases, similar experiments were performed with $q_1 = 40$ mm and $q_1 = 50$ mm. The graph of measured output angle θ for various values of applied torques at the three chosen values of q_1 are shown in Fig. 5. In this figure, the observed data points at each of the three values of q_1 have been connected using straight lines obtained via the principle of least squares. The slope of each of the three straight lines thus obtained gives the values of the stiffness of the actuator at the three different values of q_1 used during the experiments. These have been found to be equal to 7.163 N-mm/deg, 13.682 N-mm/deg and 22.191 N-mm/deg at $q_1 = 28$ mm, 40 mm and 50 mm, respectively.

The maximum measured output angle during the experiments was 8.21 degrees. The stiffness of the actuator given by equation (3) is $K = 2kq_1(q_2 - l_0) \sin \theta + 2kq_1^2 \cos 2\theta$, where k denotes the stiffness of each of the springs used in the device. The stiffness of the plastic springs used in the actuator prototype is given by $k = 0.0044$ N/mm. Since the measured output angles during the experiments were small, the stiffness K of the prototype for the experimental

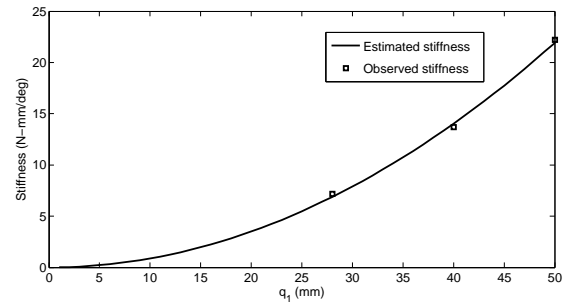


Fig. 6. Graph of actuator stiffness K vs q_1 .

conditions can be approximated as $K = 2kq_1^2$. A plot of the estimated stiffness curve using this formula and the observed values of stiffness at the three values of q_1 are shown in Fig. 6. According to this figure, there is a good agreement between the estimated and observed values of the actuator stiffness at the three values of q_1 used during the experiments.

VI. CONCLUSION

We have presented the principle, design and prototype realization of an energy-efficient rotational variable stiffness actuator. The stiffness and output angle of the prototype presented in this paper can be independently varied by means of slide screws. This implies that:

- the actuator stiffness can be varied at any output angle configuration of the actuator, keeping the output angle constant;
- the output angle of the actuator can be varied, keeping its stiffness constant.

An automatically controlled variable stiffness actuator can be developed based on the conceptual and mechanical design presented in this paper, with the help of encoders, motors and motor controllers. This actuator can be used to form the core part in clinical prosthetic devices with some means of decoding intended stiffness and position information from neural signals, and also in some automated tools for surgery where safe interaction with humans is of prime importance.

REFERENCES

- [1] S. Rao, R. Carloni and S. Stramigioli, "Stiffness and position control of a prosthetic wrist by means of an EMG interface", *IEEE International Conference Engineering in Medicine and Biology Society*, 2010.
- [2] R. Van Ham, T.G. Sugar, B. Vanderborght, K.W. Hollander and D. Lefeber, "Compliant Actuator Designs", *IEEE Robotics and Automation Magazine*, vol. 16, issue 3, pp. 81-94, 2009.
- [3] L.C. Visser, R. Carloni, R. Únal and S. Stramigioli, "Modeling and design of energy efficient variable stiffness actuators", *IEEE International Conference on Robotics and Automation*, 2010.
- [4] L.C. Visser, R. Carloni, F. Klijnstra and S. Stramigioli, "A prototype of a novel energy efficient variable stiffness actuator", *IEEE International Conference Engineering in Medicine and Biology Society*, 2010.
- [5] A. Jafari, N. Tsagarakis, B. Vanderborght and D. Caldwell, "AwAS II: A new actuator with adjustable stiffness based on the novel principle of adaptable pivot point and variable lever ratio", *IEEE Int. Conf. on Robotics and Automation*, 2011.
- [6] B-S. Kim, J-B. Song, "Hybrid Dual Actuator Unit: A design of a variable stiffness actuators based on an adjustable moment arm mechanism", *IEEE Int. Conf. on Robotics and Automation*, 2010.